Journal of Solid State Electrochemistry (2019) 23:1851–1860
https://doi.org/10.1007/s10008-019-04206-8

ORIGINAL PAPER

One-pot synthesis of P-toluidine-reduced graphene oxide/Mn_3O_4 composite and its electrochemical performance

Nali Chen[1,2] · Daipeng Hu[1] · Yueyi Wang[1] · Lin Tan[1] · Feifei Zhang[1] · Huixia Feng[1,2]

Received: 7 May 2018 / Revised: 20 January 2019 / Accepted: 26 January 2019 / Published online: 11 May 2019

Abstract

In this paper, a promising electrode material for supercapacitor based on P-toluidine-reduced graphene oxide/Mn_3O_4 (GM) composite was successfully synthesized through a new one-pot synthesis route. To obtain GM composite, graphite oxide (GO) was reduced by P-toluidine first, and then, the resulting reduced graphene oxide (RGO) was hydrothermally treated accompanied with $KMnO_4$ and K_2SO_4. The effect of K_2SO_4 on the microstructure and electrochemical performance of as-synthesized composites was investigated. At the weight feed ratio of the theoretical amount of Mn_3O_4 to GO is 13:1, the GM composite prepared with K_2SO_4 displays a network structure, but under the same conditions, GM composite prepared without K_2SO_4 presents a different-sized lumps structure closely piled up by Mn_3O_4 nanoparticles. A specific capacitance of the GM composite prepared with K_2SO_4 reaches to 331.6 F/g, almost two times higher than that of the composite prepared without K_2SO_4. Moreover, the specific capacitance retention of the composite is above 88% after 1000 cycles at 5.0 A/g.

Keywords Graphite oxide · Graphene/Mn_3O_4 · Mn_3O_4 · K_2SO_4 · Supercapacitors

Introduction

Supercapacitors have received extensive attention and much interest due to their high power density, fast charge-discharge rate, and long life cycle [1]. The component, structure, and surface morphology of electrode materials for supercapacitors largely determine their performance [2]. Manganese oxides are attractive electrode materials for supercapacitors because of the large theoretical specific capacitance, high abundance of Mn element, environmental benignity, and rich redox manganese valences (Mn^{2+}, Mn^{3+}, Mn^{4+}, etc.) [3–8]. The capacitive performance of manganese oxides is realized from the oxidation-reduction process at electrode surfaces. Mn_3O_4 with low-cost, low-toxicity, and simple synthesis process is a kind of manganese oxide and an ideal electrode material for supercapacitors [9]. However, the specific capacitance of pure Mn_3O_4 is low resulting from the poor electric conductivity and low electron transport rate. Therefore, improving the conductivity of Mn_3O_4 is an effective way to enhance its specific capacitance [10]. Carbon materials (graphene [11, 12], carbon nanotube [7, 13], carbon aerogel [14], activated carbon [15], etc.), which store electrical energy via an electrostatic charge storage mechanism on their surfaces, have a high electrical conductivity [3, 16]. Combining carbon materials with Mn_3O_4 can result in a carbon/Mn_3O_4 composites with outstanding electrochemical performance [3, 5, 9, 17, 18].

Graphene, a kind of 2-dimension monolayer of carbon atoms arranged in a hexagonal lattice, has an excellent electrical conductivity, large surface area, and has become an ideal substrate to grow and anchor nanomaterials. Therefore, graphene/Mn_3O_4 (sometimes called "reduced graphene oxide/Mn_3O_4") (GM) composites have been prepared by various methods. Zhang et al. [19] synthesized GM composite with Mn_3O_4 nanoparticles anchored to graphene nanosheets by one-step solvothermal method using dimethyl sulfoxide as solvent, and the as-synthesized composite exhibited a specific capacitance of 147 F/g. Fan et al. [10] reported a facile one-step hydrothermal method to synthesize GM composite with a specific capacitance of 171 F/g using hydrazine hydrate as reductant for graphite oxide (GO). Xu et al. [20] developed an atom-economic way to prepare GM composite, which

✉ Nali Chen
chennl2007@126.com

✉ Huixia Feng
fenghx1966@163.com

[1] College of Petrochemical Technology, Lanzhou University of Technology, Lanzhou 730050, China

[2] State Key Laboratory of Advanced Processing and Recycling of Nonferrous Metals, Lanzhou University of Technology, Lanzhou 730050, China

included the hydrothermal reduction of GO/$MnSO_4$ suspension produced via Hummers method, and then the preparation of GM composite. The as-prepared GM composite obtained a specific capacitance of 186.2 F/g. The specific capacitance of the above-mentioned GM composites is not still very satisfying when the composites are applied in supercapacitors. Until recently, Zhang et al. [21] successfully prepared GM composite with a high specific capacitance of 326.9 F/g and a good cycle stability of 94.6% retention after 1000 cycles from the precursor of GO/MnO_2 via hydrothermal reaction assisted by dilute hydrazine hydrate. However, the preparation of precursor of GO/MnO_2 was first required, and the hydrazine hydrate is poisonous, environmental, detrimental, and explosive. A facile and environmental-friendly method for the preparation of GM composite is still desired.

Recently, Jin's group and our group reported that GO could be successfully converted into reduced graphene oxide (RGO) by aniline [22, 23]. Compared with aniline, P-toluidine contains a weak electron-donating substituent group methyl and has a stronger reducing action. Meanwhile, the activity of the electrode material is mainly dependent on the microstructure of the active material. The microstructure of manganese oxide is affected by the salt modifiers under hydrothermal conditions [24]. In this paper, GM composites were prepared by a new facile one-pot method that including the reduction of GO by P-toluidine and then the hydrothermal treatment of the resulting RGO dispersion accompanied with $KMnO_4$ as Mn source and K_2SO_4 as modifier. It only took 1 h to convert GO into RGO with P-toluidine as reductant. The effect of K_2SO_4 on the microstructure and the electrochemical performance of the resulting composites was investigated. The microstructures of GM composites were characterized by X-ray diffraction (XRD), X-ray photoelectron spectroscopy (XPS), scanning electron microscope (SEM), and transmission electron microscope (TEM). The electrochemical performance of GM composites was measured by the cyclic voltammetry (CV), galvanostatic charge-discharge (GCD), and electrochemical impedance spectroscopy (EIS) in a 1 M Na_2SO_4 aqueous solution. At the weight feed ratio of the theoretical amount of Mn_3O_4 to GO is 13:1, GM composite prepared with K_2SO_4 displays a network structure and a high specific capacitance (331.6 F/g), but under the same conditions, GM composite prepared without K_2SO_4 presents a different microstructure and a lower specific capacitance of 179.7 F/g.

Experiment

Materials

For the preparation of GM composites, natural graphite, $KMnO_4$, P-toluidine, K_2SO_4, etc., were purchased from Laiao Chemical Reagents Company, Gansu. All reagents were analytical grade and used without further purification. All solutions were prepared with distilled water.

Preparation of GO suspension

GO was prepared by modified Hummers' method as described elsewhere [23]. Briefly, concentrated H_2SO_4 (50 mL), natural graphite (1.0 g), and $NaNO_3$ (1.0 g) were added into a 250-mL flask placed in an ice bath. $KMnO_4$ (6.0 g) was slowly added into the solution with stirring below 5 °C for 2 h. Then, the mixture was stirred for another 30 min at 35 °C. After that, excess distilled water was added into the above mixture; the temperature was allowed to rise to 90 °C and the mixture was stirred for 30 min. A deep brown mixture was obtained. Finally, 30% H_2O_2 aqueous solution was added to the deep brown mixture until the color of the mixture changed into brilliant yellow. The resulting suspension was filtered while it was still hot, washed with 5% HCl in succession five times and removed metal ions by dialysis for a week. Finally, the resulting GO slurry was dispersed in distilled water to prepare GO suspension.

Preparation of GM composites

GM composites were prepared by one-pot method shown in Fig. 1. In a typical synthesis, 0.05 g p-toluidine was added to the abovementioned suspension containing 0.01 g GO, and the mixture was sonicated for 30 min followed by stirring in 95 °C water bath. After stirring for 1 h, a black RGO dispersion was obtained. Afterwards, 40 mL aqueous solution with 0.2726 g $KMnO_4$ and 0.3002 g K_2SO_4 (n ($KMnO_4$):n (K_2SO_4) = 1:1) was added to the resulting RGO dispersion. The resulting mixture was stirred for 1 h followed by transferring into Teflon-lined autoclave. The autoclave was sealed and heated in an oven at 140 °C for 2 h. Then, the autoclave was cooled to room temperature. Finally, the product was collected by centrifugation, washing with distilled water, and drying overnight at 60 °C. The abbreviated name of as-prepared product was GM13/SOP composite. Composites were also

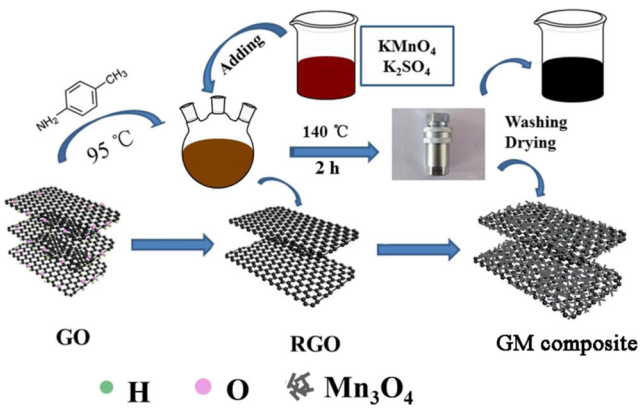

Fig. 1 Schematic illustration of the preparation of GM composites

prepared with the weight feed ratios of the theoretical amount of Mn_3O_4 to GO of 6.5:1, 22:1, and 35:1, and as-prepared composites were named as GM6.5/SOP, GM22/SOP, and GM35/SOP, respectively.

In order to investigate the effect of K_2SO_4 on the microstructure and the electrochemical performance of the resulting composites, the composites named by GM6.5, GM13, GM22, and GM35 were respectively prepared through the abovementioned procedure for the preparation of GM6.5/SOP, GM13/SOP, GM22/SOP, and GM35/SOP only without K_2SO_4.

Characterization

The crystallographic structure of the samples was confirmed by a XRD (XRD-6000, Shimadzu Co., Ltd. Tokyo, Japan) equipped with Cu-K_α as a radiation source ($\lambda = 1.5406$ Å). Each sample was scanned in the range of 5–80° with a step size of 0.02°. XPS measurement was carried out on a VG scientific ESCA-300 spectrometer with non-monochromatized Mg Kα radiation. The morphology and size of the as-prepared samples were characterized with SEM (S-4300, Hitachi Co., Ltd. Tokyo, Japan) and TEM (H-8110, Hitachi Co., Ltd. Tokyo, Japan). For this purpose, dispersions of composites were pipetted onto carbon-coated copper grids.

Electrochemical measurements

All electrochemical measurements were conducted with CHI660E electrochemical workstation (Shanghai Chenhua Instrument, China) using a three-electrode cell in a 1 M Na_2SO_4 aqueous solution. The platinum wire electrode and the saturated calomel electrode (SCE) were used as counter and reference electrode, respectively. The work electrodes were prepared by the following procedure. The active materials, acetylene black, and polytetrafluoroethylene (PTFE) emulsion were mixed in a mass ratio of 85:10:5. Then, the mixture was grinded and dispersed in anhydrous ethanol to produce a homogeneous paste. Finally, the paste was casted onto the treated stainless steel mesh (effective area 1 × 1 cm^2), dried under vacuum at 60 °C for 12 h, and pressed at 10 MPa.

CV and GCD measurements were performed within a potential window from − 0.2 to 0.8 V (vs. SCE). EIS was measured in a frequency range of 100 to 0.01 kHz with voltage amplitude of 5 mV. The specific capacitance was calculated from the discharge curve according to the following Eq. (1):

$$C_m = \frac{I \times t}{\Delta V \times m} \quad (1)$$

Where C_m (F/g) is the specific capacitance, I (A) is the discharge current, t (s) is the discharge time, ΔV (V) is the potential range during discharge process, and m (g) is the mass of active material in work electrode.

Results and discussion

Material characterization

XRD was used to analyze the reduction of GO and the formation of GM composites. Figure 2 shows the XRD patterns of GO, GM6.5/SOP, GM13/SOP, and GM13 composites. The sharp peak at $2\theta = 10.8°$ in the XRD pattern of GO corresponds to the increased interlayer spacing of 0.815 nm, which is due to the formation of oxygen functionalities on the surface of graphene sheets, indicating the successful oxidation of natural graphite [23, 25, 26]. The appearance of a small peak centered at $2\theta = 22°$ can be ascribed to the presence of a small amount of unreacted graphitic carbon in GO [27]. For GM composites, the sharp peak at $2\theta = 10.8°$ disappears, confirming the partial reduction of GO in GM composites [4]. For GM6.5/SOP composite, sharp diffraction peaks are

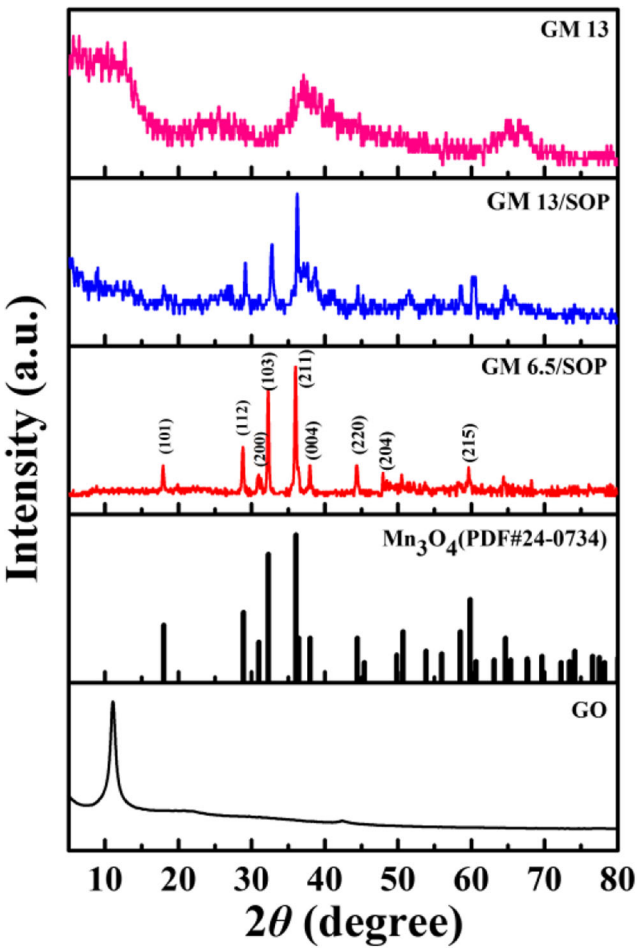

Fig. 2 XRD patterns of the GO (**a**), JCPDS no. 24-0734 (**b**), GM6.5/SOP (**c**), GM13/SOP (**d**), and GM13 (**e**) composites

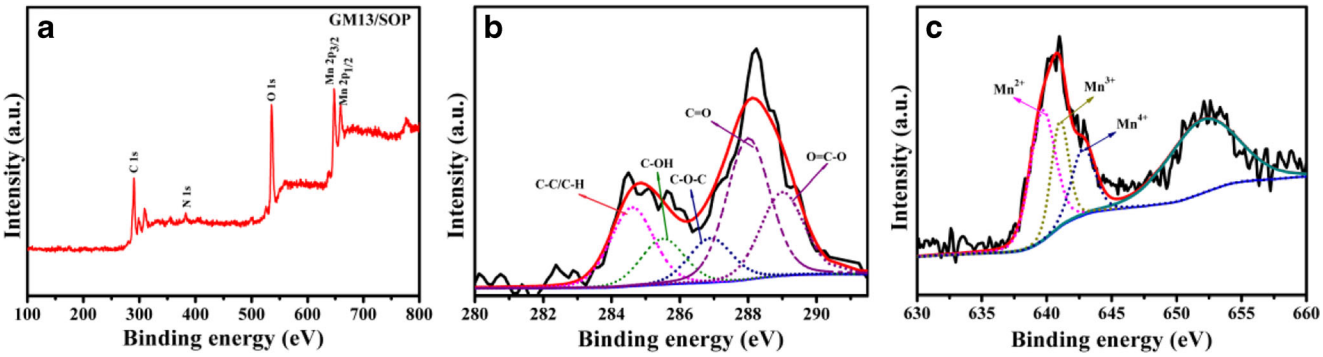

Fig. 3 Wide scan survey (a), C 1 s (b), and Mn 2p (c) XPS spectra of GM13/SOP composite

observed at 2θ values of 18°, 28.88°, 31.01°, 36.08°, 37.98°, 44.44°, 49.82°, and 60.63°, which have been well matched with the standard XRD pattern of Mn_3O_4 (JCPDS no. 24-0734), corresponding to the (101), (112), (200), (103), (211),

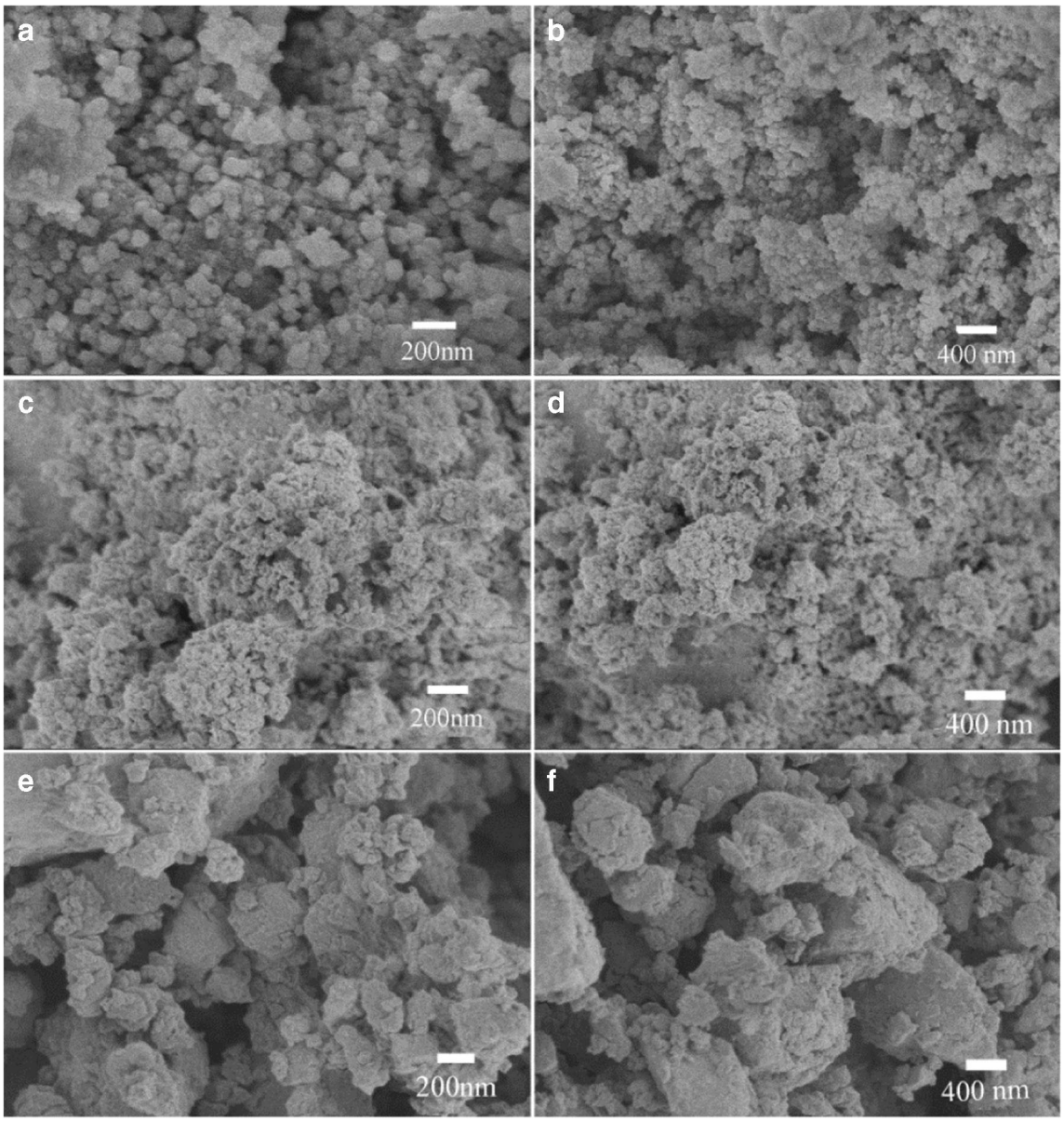

Fig. 4 SEM images of GM6.5/SOP (**a**, **b**), GM13/SOP (**c**, **d**), and GM13 (**e**, **f**) composites

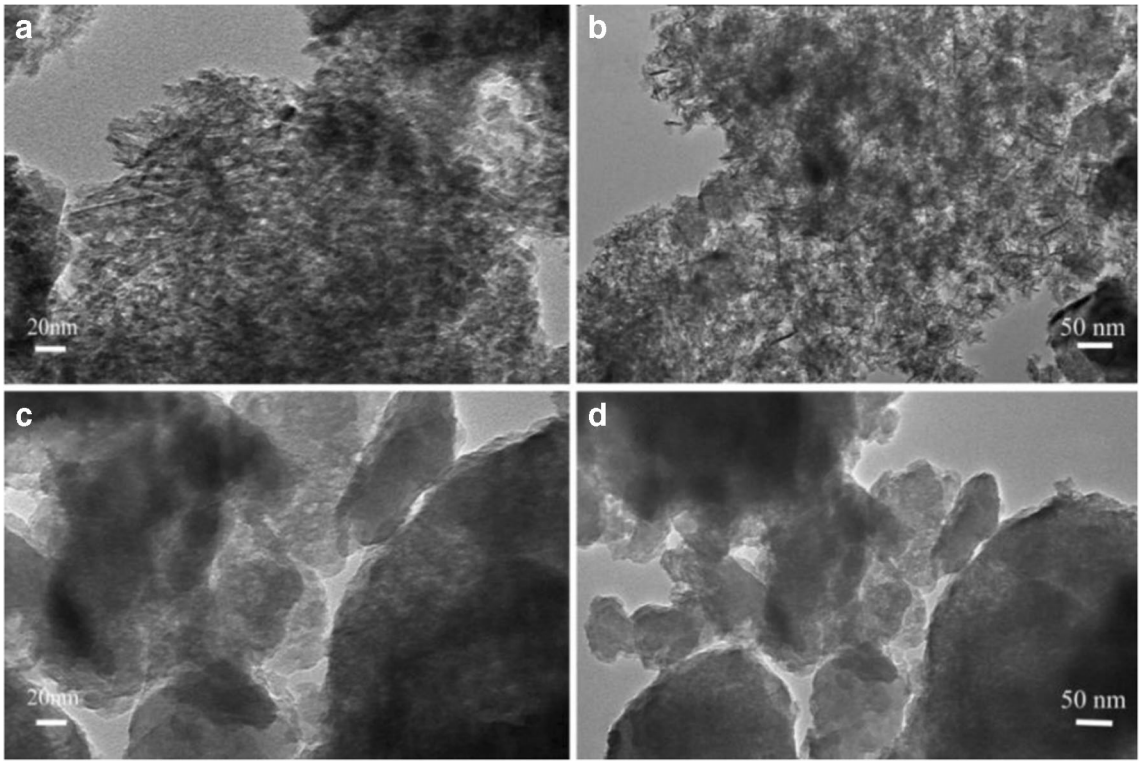

Fig. 5 TEM images of GM13/SOP composite (**a**, **b**) and GM13 composite (**c**, **d**)

(004), (220) and (204) reflections, respectively. These phenomena demonstrate that the GM composite was successfully synthesized [6, 28, 29].

The XRD pattern of GM13/SOP composite also shows diffraction peaks at $2\theta = 18°$, 28.88°, 31.01°, 36.08°, 37.98°, 44.44°, 49.82°, and 60.63°, which is basically similar to that of GM6.5/SOP composite. However, it is also noted that the intensity of diffraction peaks is weaker than that of GM6.5/SOP composite, and even some weak diffraction peaks disappear. The low intensity and broad width of the diffraction peaks of GM13/SOP composite should be related to weak crystalline Mn_3O_4 in composite [30] . The increased crystallization degree can improve the stability of electrode material, but is not beneficial to the charge transportation [31]. Therefore, weak crystalline Mn_3O_4 in GM13/SOP composite was expected to deliver a higher energy storage. Compared with GM13/SOP composite, GM13 composite presents a different XRD pattern. Broad and weak diffraction peaks for GM13 composite are observed at $2\theta = 36.08°$ and 65.39°, which are respectively ascribed to (211), (323) lattice planes of Mn_3O_4 by referring to the JCPDS no. 24-0734. The broad peaks are related to a low crystallinity. This indicates that K_2SO_4 has a significant impact on the crystallinity of Mn_3O_4 in GM composite.

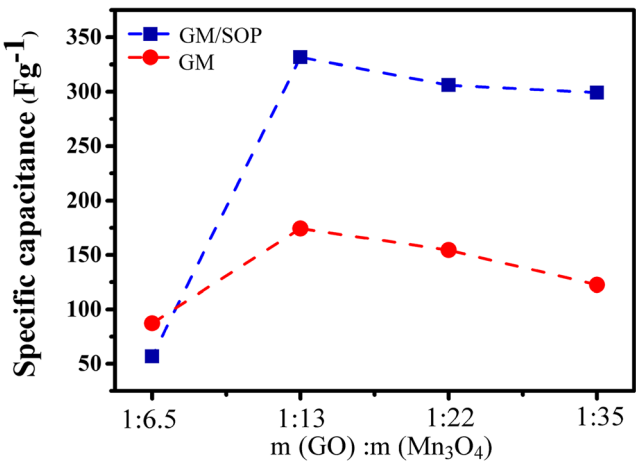

Fig. 6 The specific capacitance of GM/SOP and GM composites prepared from different weight feed ratios of the theoretical amount of Mn_3O_4 to GO at a current density of 0.1 A/g

XPS has been used to further confirm the successful synthesis of GM13/SOP composite. Figure 3a was a wide scan survey of GM13/SOP composite; the percent of C element was 48.61%; O was 39.24%; Mn was 12.15%. Figure 3b shows the C 1 s XPS spectrum of GM13/SOP composite. The C 1 s XPS spectrum of the composite shows five different peaks centered at 284.6, 285.5, 286.9, 288, and 289.0 eV, which are corresponding to C-C/C-H, C-OH, C-O-C, C = O, and O = C-O groups, respectively [9, 19, 21]. The Mn 2p XPS spectrum (Fig. 3c) presents spin-orbit splitting into 2p1/2 and 2p3/2 components, corresponding to the different binding energy of 652.5 and 640.8 eV with energy splitting of 11.7 eV. Obviously, three components of Mn 2p3/2 peak with the

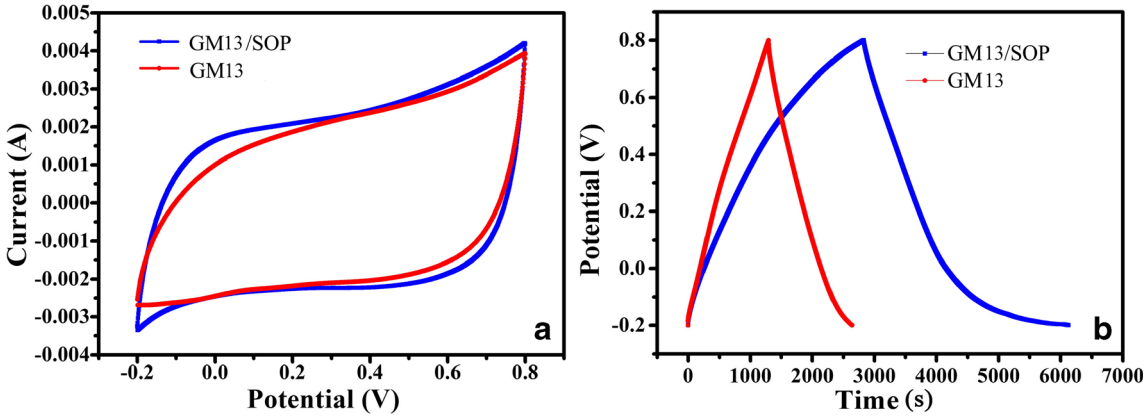

Fig. 7 CV (**a**) and GCD (**b**) curves of GM13/SOP and GM13 composites

binding energy of 640.7, 641.7, and 642.6 eV can be observed, which are assigned to Mn^{2+}, Mn^{3+}, and Mn^{4+} cations, respectively [32, 33].

Morphology of GM6.5/SOP, GM13/SOP, and GM13 composites was investigated by SEM and TEM, and the results are shown in Figs. 4 and 5. It can be seen from Fig. 4a, b that flake-like Mn_3O_4 nanoparticles are anchored on the surface of RGO sheets for GM6.5/SOP composite. The morphology of Mn_3O_4 nanoparticles is similar to that of the Mn_3O_4 nanoparticles synthesized previous work [10]. With the increase of $KMnO_4$ and K_2SO_4 amount, the composite presents a diverse morphology. From Fig. 4c, d and Fig. 5a, b, we can note that GM13/SOP composite displays a network structure that formed by interweaving nanothreads of Mn_3O_4 on the surface of RGO sheets.

Meanwhile, the morphology of composite also changes without K_2SO_4. The SEM and TEM images of GM13/SOP and GM13 composites clearly present the effect of K_2SO_4 on the Mn_3O_4 crystals growth and the morphology of composite. The image of GM13 composite displays a different-sized lumps structure closely piled up by Mn_3O_4 nanoparticles (see Fig. 4e, f and Fig. 5c, d). With the introduction of K_2SO_4, the dispersion of composite becomes more uniform, and the network structure formed by the randomly cross-linked nanothreads on the surface of RGO sheets is clearly observed (see Fig. 4c, d and Fig. 5a, b). Combining of the XRD, we can find GM13/SOP composite displays a different microstructure from those of GM6.5/SOP and GM composites. The main reasons are originated from two factors: one is the increase of $KMnO_4$ amount, and the other is the introduction of K_2SO_4. To be specific, the reaction rate between $KMnO_4$ and RGO increases with the increase of $KMnO_4$ amount. Thus, a lot of Mn_3O_4 were formed in a short time as the amount of $KMnO_4$ increased, and the crystallinity decreased and the morphology changed. Simultaneously, the introduction of K_2SO_4 affected the crystal growth and the formation rate of manganese oxide [24] and changed the microstructure of GM composite. Therefore, K_2SO_4 played a crucial role during the synthesis of GM13/SOP composite with unique network structure. The effect mechanism of K_2SO_4 is complicated. We will try further to gain more information for the deeper research. The unique network structure of GM13/SOP composite is helpful to improve the efficiency of ion transportation and reduce the ion diffusion path [34]. These characters will result in an improvement of the electrochemical performance of composite in some extent. In addition, the network structure of GM13/SOP composite can provide a large specific surface area, which is also beneficial to its electrochemical performance improvement [25].

Electrochemical measurements

The specific capacitance of GM/SOP and GM composites prepared with different weight feed ratios of the theoretical amount of Mn_3O_4 to GO was calculated by Eq. (1) and is shown in Fig. 6. As shown in Fig. 6, the specific capacitance

Table 1 The comparison of the specific capacitance of the reported graphene/Mn_3O_4 composites

Samples	Specific capacitance/F/g	Electrolyte	Report
Graphene/Mn_3O_4	147 (− 0.1–0.8 V, 0.1 A/g)	1 M Na_2SO_4	[19]
Mn_3O_4/graphene	171 (− 0.2–0.8 V, 0.1 A/g)	1 M Na_2SO_4	[10]
Mn_3O_4/graphene	270.6 (− 0.2–0.8 V, 0.2 A/g)	1 M Na_2SO_4	[39]
Mn_3O_4/graphene	312 (− 0.1–0.9 V, 0.5 mA/cm^2)	1 M Na_2SO_4	[25]
GM13/SOP	331.6 (− 0.2–0.8 V, 0.1 A/g)	1 M Na_2SO_4	This work

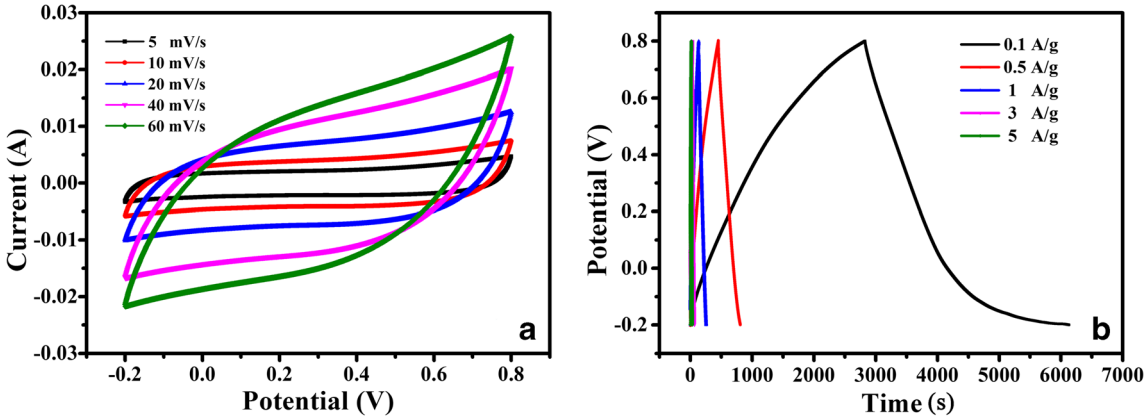

Fig. 8 CV (**a**) curves of GM13/SOP composite at different scan rates (5, 10, 20, 40, and 60 mV/s) and GCD (**b**) curves of GM13/SOP composite at different current densities (0.1, 0.5, 1, 3, and 5 A/g)

of composites first increases, and then decreases with the increase in the weight feed ratio of the theoretical amount of Mn_3O_4 to GO. The decrease in specific capacitance of composites at a high weight feed ratio is ascribed to the agglomeration of excessive amount of Mn_3O_4. For GM/SOP and GM composites, the specific capacitance all reaches the maximum value at the 13:1 of the weight feed ratio of the theoretical amount of Mn_3O_4 to GO, and the specific capacitance of GM13/SOP composite (331.6 F/g) is higher than that of GM13 composite (179.7 F/g). In order to further investigate the effect of K_2SO_4 on the electrochemical performance of composites, the GM13/SOP and GM13 composites were selected and studied in detail.

The CV curves of GM13/SOP and GM13 composites at a scan rate of 5 mV/s are shown in Fig. 7a. It is noted that the CV curves of GM13/SOP and GM13 composites are an approximating rectangular shape, showing the ideal capacitive behavior [6, 35]. In addition, it is also observed that there is no clear redox peak in CV curves. The explanation for the phenomenon focuses on that the electrode is charged and discharged at a constant rate over the complete cycle [36]. The large loop area of the CV curve indicates a high specific capacitance [30, 37]. Therefore, the loop area of the CV curve of GM13/SOP composite is larger than that of GM13 composite, indicating a higher specific capacitance for GM13/SOP composite. This is attributed to its network structure, which can provide efficient ion transportation, short ion diffusion path, and large specific surface area [37, 38].

The GCD measurements were used to evaluate the electrochemical performance of GM13/SOP and GM13 composites at a current density of 0.1 A/g, and the results are shown in Fig. 7b. In comparison with GM13 composite, GM13/SOP composite presents a longer discharging time, indicating a higher specific capacitance for GM13/SOP composite. The value of specific capacitance calculated by Eq. (1) and curves of GCD is 331.6 and 179.7 F/g for GM13/SOP and GM13 composites, respectively. This is in good agreement with the deduced result from the CV curves. The specific capacitance of GM13/SOP composite is also higher than that of graphene/Mn_3O_4 composites in previous reports, as presented in Table 1.

The rate capability is an important factor for GM13/SOP composite as electrode material of supercapacitors. Therefore, the CV curves of GM13/SOP composite at different scanning rates (from 5 to 60 mV/s) were tested and are displayed in Fig. 8a. It is noted that the curve at 20 mV/s shows a similar shape to that at 5 mV/s, and the current response significantly increases with the increase of scan rate, which indicate a good rate capability for GM13/SOP composite. The GCD curves of GM13/SOP composite at various current densities are shown in Fig. 8b. The specific capacitance of composites at different current densities is shown in Table 2. The specific capacitance decreases in company with the increase of current density [38]. According to Table 2, the specific capacitance of GM13/SOP composite at the current density of 0.1 and 0.5 A/g is respectively 331.6 and 224.2 F/g, higher than that

Table 2 The specific capacitance of GM/SOP and GM13 composites at different current densities

Current density (A/g)	Specific capacitance (F/g)				
	GM6.5/SOP	GM13/SOP	GM22/SOP	GM35/SOP	GM13
0.1	56.9	331.6	301.6	294.9	174.4
0.5	40.2	224.2	202.9	176.0	141.9
1	32.2	152.4	182.0	145.3	108.7

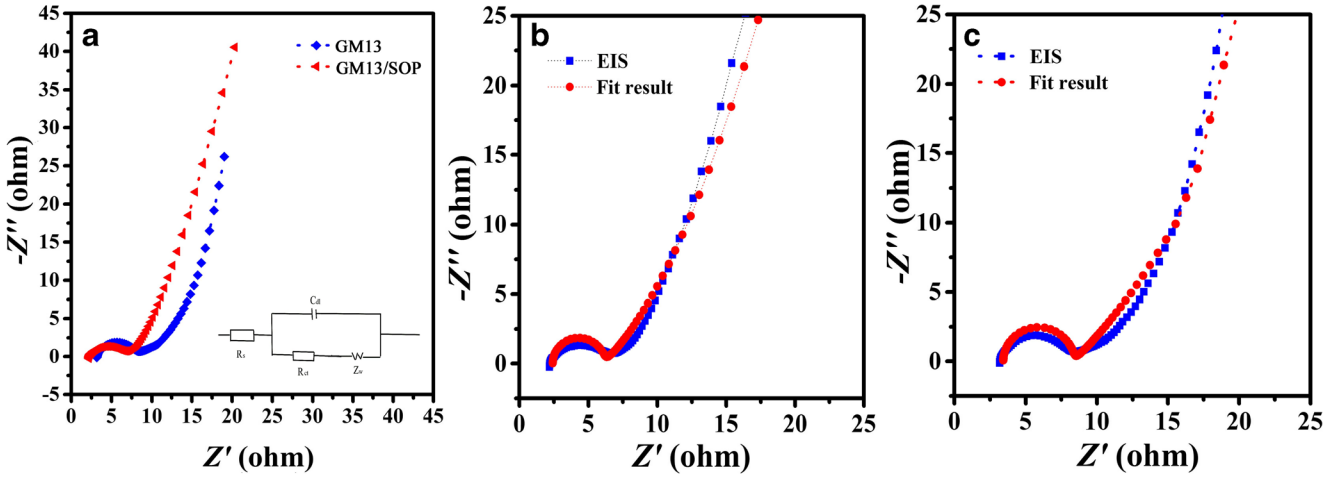

Fig. 9 Nyquist plots of GM13/SOP and GM13 composites (**a**) and Z-view fitted Nyquist plots of GM13/SOP (**b**) and GM13 (**c**) composites; the inset shows the corresponding equivalent circuit

of other GM/SOP composites at the same current density. It is noted that GM13/SOP composite also presents a higher specific capacitance than GM13 composite at the same current density.

Figure 9a shows the Nyquist plots of GM13/SOP and GM13 composites. To exemplificatively understand the Nyquist plots, the results of plots were fitted with the equivalent circuit as shown in the inset of Fig. 9a. The fitted results are shown in Fig. 9b, c. The fitting values and chi-square statistics are presented in Table 3. Principally, four components of equivalent circuit are defined to describe the electrochemical capacitive characteristic, which are of the resistance of solution (R_s), electrochemical double layer (C_{dl}), charge transfer resistance (R_{ct}), and Warburg element (W) [6, 9]. It can be seen that the R_s value for GM13/SOP and GM13 composites is respectively 2.020 and 3.231 Ω, and GM13/SOP composite shows a lower R_s value, which can be attributed to the easier migration of electrolytic ions through the active surface of GM13/SOP electrode [40]. The diameter of the semicircle in the high frequency region indicates charge transfer resistance (R_{ct}) at the electrode/electrolyte interface [9, 41]. GM13/SOP composite has a resistance (R_{ct}) of 3.665 Ω, which is also lower than that of GM13 composite (4.886 Ω). The C_{dl} of the circuit is assigned to the RGO of GM composite [27]. GM13 composite has a C_{dl} of 2.287×10^{-5} F, which is lower than 5.944×10^{-5} F for GM13/SOP composite. It is anticipated that the GM13/SOP composite with the cross-linked Mn_3O_4 nanothreads homogeneously distributing on the surface of RGO sheets can supply a hybrid electrochemical environment and improve the electrode-electrolyte interaction [27]. The approximately vertical line in the low frequency region represents an ideal capacitive behavior [34] and low diffusion resistance of electrolytic ions in the electrode materials. GM13/SOP composite shows a more vertical line and a lower Warburg resistance (W) value, indicating it obtained a good capacitive behavior and facile electrolyte diffusion.

Table 3 Z-view fitted values of R_s, R_{ct}, C_{dl}, and W from the equivalent circuit corresponding to Fig. 9

Sample	R_s (Ω)	C_{dl} (F)	R_{ct}(Ω)	W
GM13	3.231	2.287×10^{-5}	4.886	0.1831
GM13/SOP	2.020	5.944×10^{-5}	3.665	0.1728

The charging/discharging cycle-life of GM13/SOP and GM13 composites was also evaluated at a current density of 5 A/g in the potential ranging from − 0.2 to 0.8 V during 1000 times and the result is shown in Fig. 10. As can be seen from Fig. 10, the specific capacitance of GM13 composite retains 82% of its initial specific capacitance after 1000 cycles. While, GM13/SOP composite exhibits a higher specific capacity retention, retaining over 88% of its initial specific capacitance after 1000 cycles. The network structure of GM13/SOP composite is helpful to improve the efficiency of ion transportation, reduce the ion diffusion path, and prevent the structure

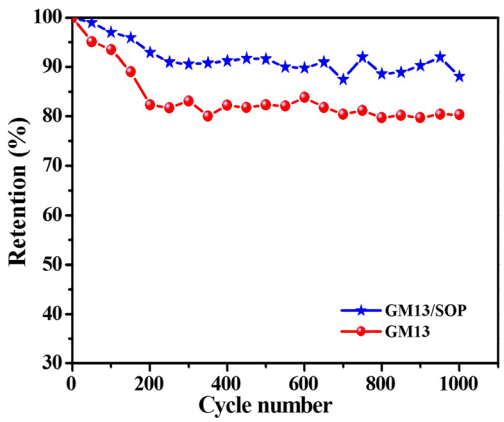

Fig. 10 Cycle life tests of GM13/SOP and GM13 composites at a current density of 5 A/g

collapse of composite during charge/discharge for 1000 cycles.

Conclusion

In summary, a new facile one-pot synthesis route to synthesis GM composite has been developed. The route included the reduction of GO with P-toluidine as reductant and then hydrothermal treatment of resulting RGO dispersion accompanied with $KMnO_4$ and K_2SO_4. K_2SO_4 has a significant influence on the microstructure and electrochemical performance of the GM composite. GM13/SOP composite obtains the maximal specific capacitance (331.6 F/g), a lower charge-transfer, and diffusive resistance, which might be attributed to its network structure. But, GM13 composite delivers a specific capacitance of 179.7 F/g, reduce by 45.8%. Furthermore, the specific capacitance retention of GM13/SOP composite reaches above 88% after 1000 cycles at a current density of 5 A/g. These results show that GM13/SOP composite is a promising candidate as electrode material for supercapacitors.

Funding information This study is financially supported by the National Natural Science Foundation of China (NSFC. 21664009, 51063003), the Ministry of Science and Technology project (No. 2009GJG10041), the Fundamental Research Funds for the Universities of Gansu (No. 1105ZTC136), the Natural Science Foundation of Gansu Province (No. 1208RJZA173).

References

1. Yu G, Hu L, Liu N, Wang H, Vosgueritchian M, Yang Y, Cui Y, Bao Z (2011) Enhancing the supercapacitor performance of graphene/MnO_2 nanostructured electrodes by conductive wrapping. Nano Lett 11(10):4438–4442
2. Kong L, Liu M, Lang J, Liu M, Luo Y, Kang L (2011) Porous cobalt hydroxide film electrodeposited on nickel foam with excellent electrochemical capacitive behavior. J Solid State Electrochem 15(3):571–577
3. Ren X (2016) Assembly of Mn_3O_4/carbon black composite and its supercapacitor application. Int J Electrochem Sci 11:5080–5089
4. Zhou H, Zhai H-J (2016) Rapid preparation of the hybrid of MnO_2 dispersed on graphene nanosheets with enhanced supercapacitive performance. Electrochim Acta 215:339–345
5. Xiao X, Wang Y, Chen G, Wang L, Wang Y (2017) Mn_3O_4/activated carbon composites with enhanced electrochemical performances for electrochemical capacitors. J Alloys Compd 703:163–173
6. Bui PTM, Song J, Li Z, Akhtar MS, Yang OB (2017) Low temperature solution processed Mn_3O_4 nanoparticles: enhanced performance of electrochemical supercapacitors. J Alloys Compd 694: 560–567
7. Chen J, Huang Y, Zhang X, Chen X, Li C (2015) MnO_2 grown in situ on graphene@CNTs as electrode materials for supercapacitors. Ceram Int 41(10):12680–12685
8. Tang Y, Chen S, Chen T, Guo W, Li Y, Mu S, Yu S, Zhao Y, Wen F, Gao F (2017) Synthesis of peanut-like hierarchical manganese carbonate microcrystals via magnetically driven self-assembly for high performance asymmetric supercapacitors. J Mater Chem A 5(8): 3923–3931
9. Song YZ, Zhao RX, Zhang KK, Ding JJ, Lv XM, Chen M, Xie JM (2017) Facile synthesis of Mn_3O_4/double-walled carbon nanotube nanocomposites and its excellent supercapacitive behavior. Electrochim Acta 230:350–357
10. Fan Y, Zhang X, Liu Y, Cai Q, Zhang J (2013) One-pot hydrothermal synthesis of Mn_3O_4/graphene nanocomposite for supercapacitors. Mater Lett 95:153–156
11. Zeng Q, Ullah Z, Chen M, Zhang H, Wang R, Gao L, Liu L, Tao G, Li Q (2017) Assembly of highly stable aqueous dispersions and flexible films of nitrogen-doped graphene for high-performance stretchable supercapacitors. J Mater Sci 52(21):12751–12760
12. Selvakumar D, Alsalme A, Alswieleh A, Jayavel R (2017) Freestanding flexible nitrogen doped-reduced graphene oxide film as an efficient electrode material for solid-state supercapacitors. J Alloys Compd 723:995–1000
13. Jin EM, Lim JG, Jeong SM (2017) Facile synthesis of graphene-wrapped CNT-MnO_2 nanocomposites for asymmetric electrochemical capacitors. J Ind Eng Chem 54:421–427
14. Pan Z, Liu M, Yang J, Qiu Y, Li W, Xu Y, Zhang X, Zhang Y (2017) High electroactive material loading on a carbon nanotube@3D graphene aerogel for high-performance flexible all-solid-state asymmetric supercapacitors. Adv Funct Mater 27(27):1701122
15. Liu R, Liu E, Ding R, Liu K, Teng Y, Luo Z, Li Z, Hu T, Liu T (2015) Facile in-situ redox synthesis of hierarchical porous activated carbon@MnO_2 core/shell nanocomposite for supercapacitors. Ceram Int 41(10):12734–12741
16. Suktha P, Phattharasupakun N, Dittanet P, Sawangphruk M (2017) Charge storage mechanisms of electrospun Mn_3O_4 nanofibres for high-performance supercapacitors. RSC Adv 7(16):9958–9963
17. Kéranguéven G, Faye J, Royer S, Pronkin SN (2016) Electrochemical properties and capacitance of Hausmannite Mn_3O_4-carbon composite synthesized by in situ autocombustion method. Electrochim Acta 222:755–764
18. Wang K, Ma X, Zhang Z, Zheng M, Geng Z, Wang Z (2013) Indirect transformation of coordination-polymer particles into magnetic carbon-coated Mn_3O_4 (Mn_3O_4@C) nanowires for supercapacitor electrodes with good cycling performance. Chemistry 19(22):7084–7089
19. Zhang X, Sun X, Chen Y, Zhang D, Ma Y (2012) One-step solvothermal synthesis of graphene/Mn_3O_4 nanocomposites and their electrochemical properties for supercapacitors. Mater Lett 68:336–339
20. Xu J, Fan X, Xia Q, Shao Z, Pei B, Yang Z, Chen Z, Zhang W (2016) A highly atom-efficient strategy to synthesize reduced graphene oxide-Mn_3O_4 nanoparticles composites for supercapacitors. J Alloys Compd 685:949–956
21. Zhang N, Qi P, Ding Y-H, Huang C-J, Zhang J-Y, Fang Y-Z (2016) A novel reduction synthesis of the graphene/Mn_3O_4 nanocomposite for supercapacitors. J Solid State Chem 237:378–384
22. Jin Y, Fang M, Jia M (2014) In situ one-pot synthesis of graphene–polyaniline nanofiber composite for high-performance electrochemical capacitors. Appl Surf Sci 308:333–340
23. Chen N, Ren Y, Kong P, Tan L, Feng H, Luo Y (2017) In situ one-pot preparation of reduced graphene oxide/polyaniline composite for high-performance electrochemical capacitors. Appl Surf Sci 392:71–79
24. Gui Y-C, Qian L-W, Qian X-F (2009) Nanometer MnO_2: hydrothermal synthesis and effect of salt modifiers on polymorph & morphology. Chinese J Inorg Chem 25:668–673
25. Raj BGS, Ramprasad RNR, Asiri AM, Wu JJ, Anandan S (2015) Ultrasound assisted synthesis of Mn_3O_4 nanoparticles anchored graphene nanosheets for supercapacitor applications. Electrochim Acta 156:127–137

26. Km A, M M, B J, Vs P, Jayalekshmi S (2017) Mn_3O_4/reduced graphene oxide nanocomposite electrodes with tailored morphology for high power supercapacitor applications. Electrochim Acta 236:424–433
27. Jana M, Saha S, Samanta P, Murmu NC, Kim NH, Kuila T, Lee JH (2017) A successive ionic layer adsorption and reaction (SILAR) method to fabricate a layer-by-layer (LBL) MnO_2-reduced graphene oxide assembly for supercapacitor application. J Power Sources 340:380–392
28. Liu J, Jiang L, Zhang T, Jin J, Yuan L, Sun G (2016) Activating Mn_3O_4 by morphology tailoring for oxygen reduction reaction. Electrochim Acta 205:38–44
29. Xiao Y, Cao Y, Gong Y, Zhang A, Zhao J, Fang S, Jia D, Li F (2014) Electrolyte and composition effects on the performances of asymmetric supercapacitors constructed with Mn_3O_4 nanoparticles-graphene nanocomposites. J Power Sources 246:926–933
30. Zhang C, Wang L, Zhao Y, Tian Y, Liang J (2016) Self-assembly synthesis of graphene oxide double-shell hollow-spheres decorated with Mn_3O_4 for electrochemical supercapacitors. Carbon 107:100–108
31. Xie Y, Ji J (2016) Synthesis and capacitance performance of MnO_2/RGO double-shelled hollow microsphere. J Mater Res 31(10): 1423–1432
32. Ramírez A, Hillebrand P, Stellmach D, May MM, Bogdanoff P, Fiechter S (2014) Evaluation of MnO_x, Mn_2O_3, and Mn_3O_4 electrodeposited films for the oxygen evolution reaction of water. J Phys Chem C 118(26):14073–14081
33. Ji F, Men Y, Wang J, Sun Y, Wang Z, Zhao B, Tao X, Xu G (2019) Promoting diesel soot combustion efficiency by tailoring the shapes and crystal facets of nanoscale Mn_3O_4. Appl Catal B Environ 242: 227–237
34. Guo WH, Liu TJ, Jiang P, Zhang ZJ (2015) Free-standing porous manganese dioxide/graphene composite films for high performance supercapacitors. J Colloid Interface Sci 437:304–310
35. Yan J, Fan Z, Wei T, Qian W, Zhang M, Wei F (2010) Fast and reversible surface redox reaction of graphene-MnO_2 composites as supercapacitor electrodes. Carbon 48(13):3825–3833
36. Lee HY, Goodenough JB (1999) Supercapacitor behavior with KCl electrolyte. J Solid State Chem 144(1):220–223
37. Samdani J, Samdani K, Kim NH, Lee JH (2017) A new protocol for the distribution of MnO_2 nanoparticles on rGO sheets and the resulting electrochemical performance. Appl Surf Sci 399:95–105
38. Li Z, Wang J, Liu S, Liu X, Yang S (2011) Synthesis of hydrothermally reduced graphene/MnO_2 composites and their electrochemical properties as supercapacitors. J Power Sources 196(19):8160–8165
39. Jin G, Xiao X, Li S, Zhao K, Wu Y, Sun D, Wang F (2015) Strongly coupled graphene/Mn_3O_4 composite with enhanced electrochemical performance for supercapacitor electrode. Electrochim Acta 178:689–698
40. Yang F, Zhao M, Sun Q, Qiao Y (2015) A novel hydrothermal synthesis and characterisation of porous Mn_3O_4 for supercapacitors with high rate capability. RSC Adv 5(13):9843–9847
41. Luo Y, Yang T, Li Z, Xiao B, Zhang M (2016) High performance of Mn_3O_4 cubes for supercapacitor applications. Mater Lett 178:171–174